

Charge-transfer processes in collisions of H^+ ions with phosphorus atoms at low energies

J.-P. Gu, G. Hirsch, and R. J. Buenker

Theoretische Chemie, Bergische Universität-Gesamthochschule Wuppertal, D-42097 Wuppertal, Germany

M. Kimura, C. M. Dutta, and P. Nordlander

*School of Allied Health Science, Yamaguchi University, Yamaguchi 755, Japan
and Department of Physics and Rice Quantum Institute, Rice University, Houston, Texas 77251*

(Received 26 May 1998)

We have carried out a theoretical investigation of charge transfer in collisions of H^+ ions with neutral phosphorus P atoms both in the ground and metastable states at collision energies below 10 keV/u and above 100 eV/u using a molecular representation. Molecular states for the PH^+ molecule are obtained by employing the *ab initio* multireference (single- and double-excitation) configuration-interaction method. In calculating charge-transfer cross sections, we have adopted the semiclassical impact-parameter method. The present charge-transfer cross sections from the ground-state P target are found to reach as large as $2 \times 10^{-15} \text{ cm}^2$ at 1 keV/u after slowly increasing from lower energies, and the contribution from $P^+(^3P)$ and $P^+(^5S^o)$ formations to the total are found to be comparable at the energy region where the cross section possesses a maximum. [S1050-2947(99)07201-7]

PACS number(s): 34.50.-s, 34.20.Mq, 34.70.+e

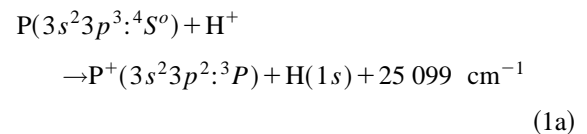
INTRODUCTION

The use of heavy ions in radiation therapy is expected to provide an advantageous therapeutic effect for tumors that are deeply seated and radioresistant, provided that an effective dose distribution can be made. In particular, at the near end of the particle track, a sharp Bragg peak is known to be present for heavy ions. This is one of their special features that is considered to be most useful for treating tumors deep inside the body [1]. An efficient exploitation of this advantage of heavy ions in radiation therapy requires a careful treatment plan that enables one to concentrate on an efficient and sufficient dose to a target region and spare surrounding critical organs. Crucial in this process is a detailed knowledge of the physical and biological properties of the charged particle beam. For this purpose, a knowledge of collision dynamics and corresponding information about collisional cross sections constitutes one of the most essential parts of radiation therapy research.

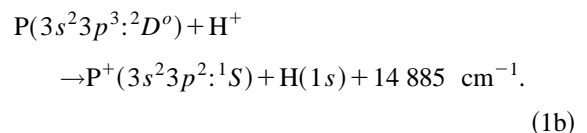
Furthermore, collisional studies involving these heavy particles are important for other fields of fundamental and applied sciences ranging from low-temperature plasma processing to astrophysics. For example, the present $H^+ + P$ collision system is of potential interest for the hydrogen envelope of Supernova 1987A. Also, the system is of importance for providing basic knowledge for heavy-ion radiation therapy, for which a facility was recently completed and an experimental treatment was initiated in Japan. However, unfortunately, studies for heavy ions have been rare due to a fundamental difficulty in correctly treating multielectronic states of such systems.

As a part of our series of studies for heavy-particle collisions [2–4], we have investigated charge transfer and excitation of phosphorus (P) atoms in collision with H^+ ions at low-to-intermediate collision energies based on a molecular expansion method. Phosphorous atoms are relatively abundantly present in general biological systems including human

bones, and a knowledge of the interaction with particles and external fields is crucial and urgently needed for therapeutic applications. The processes in which we are interested are shown, together with the corresponding asymptotic energy defects: (i) ground-state P atoms,



and (ii) metastable-state P atoms,



The metastable $^2D^o$ state of phosphorus atoms, which lies at $11\,362 \text{ cm}^{-1}$ above the ground state, is easily produced by external fields and impinging particles in various natural environments. Therefore, process (1b) competes with process (1a). In particular, experimental atomic beams produced by electron impact ionization and dissociation technique often produce a mixture of unknown amounts of the ground and excited states for open-shell atoms and hence, knowledge of individual charge-transfer cross sections may, therefore, be helpful in analyzing experimental measurements.

THEORY

Molecular states

In the present configuration interaction (CI) calculations, the atomic orbital (AO) basis set employed for the phosphorus atom is $(12s9p)$ contracted to $[6s5p]$ [5] and

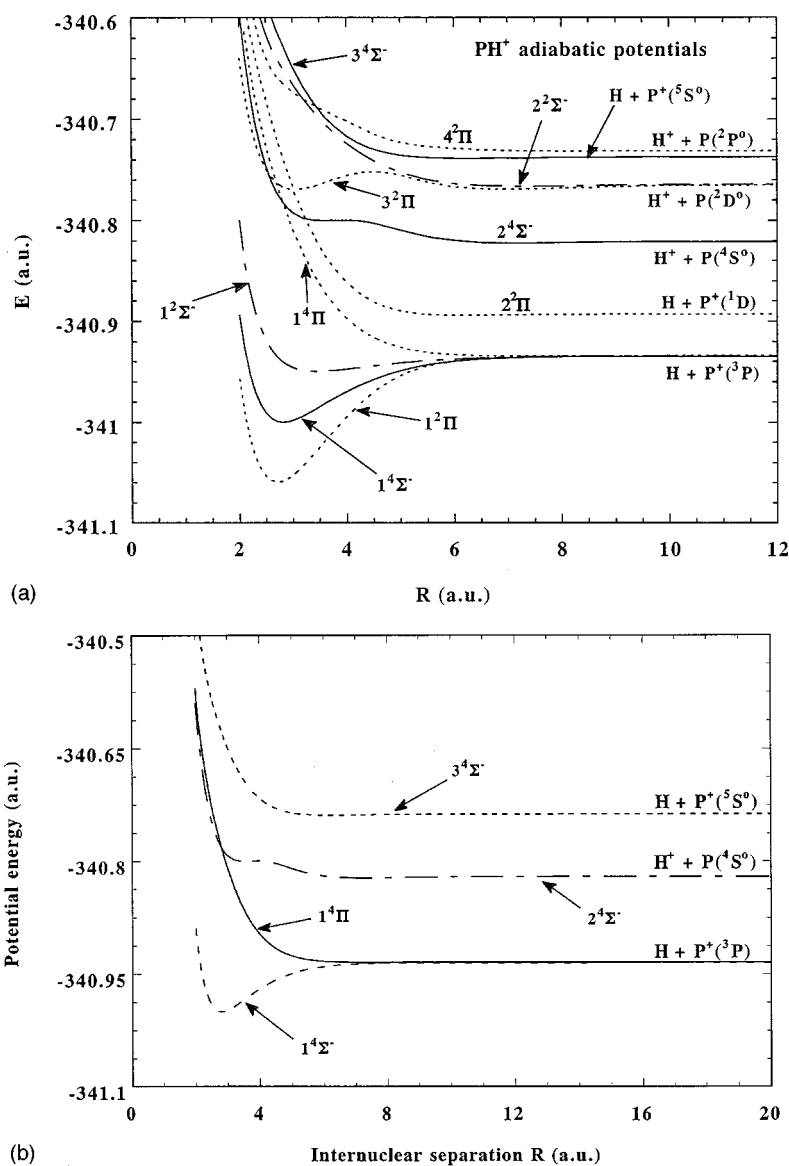


FIG. 1. The adiabatic potentials of the PH^+ molecule obtained by the present configuration-interaction calculations; (a) all related states ($^2\Sigma^+$ and $^2\Delta$ states are not included) and (b) quartet manifold.

augmented by s -, p' -, and d -type diffuse functions [6] and two d and one f polarization functions [7]. The basis set for the hydrogen atom is a $(7s3p1d)/[5s3p1d]$ contracted set that is the same as that used in Ref. [8], but one more d -type function with an exponent of 1.0 has been added. The first step in the theoretical procedure is to carry out a self-consistent-field calculation using the above AO basis sets to generate molecular orbitals (MOs), which are employed as an orthonormal basis for a multireference single- and double-excitation (MRD-CI) configuration-interaction treatment [9]. For this purpose, a set of reference configurations is chosen based on their contributions to the states of interest. All single and double excitations with respect to the reference space are generated and selected using a perturbative treatment to form secular matrices, which are then diagonalized to obtain the desired energy eigenvalues and eigenfunctions. A selection threshold [9] of $T=0.2 \times 10^{-6}$ hartree is employed at each R value. An energy extrapolation procedure [9] is also employed to account for the contribution of unselected configurations. The resulting multireference (MRD-

CI) procedure is carried out at increments of $0.1a_0$ in the $(2.0-3.6)a_0$ range of P-H separations and then at larger increments out to values as large as $8.0a_0$. The Table CI algorithm [10] is employed to handle the complicated open-shell relationships that arise in computing many-electron Hamiltonian matrix elements. The resulting electronic wave functions are subsequently employed to compute various quantities such as electric dipole and rotational matrix elements as well as nonadiabatic coupling elements involving nuclear derivatives [11].

Collision dynamics

A semiclassical MO expansion method with a straight-line trajectory of the incident ion was employed to study the collision dynamics below 10 keV [12]. In this approach, the relative motion of heavy particles is treated classically, while electronic motions are treated quantum mechanically. The total scattering wave function was expanded in terms of products of a molecular electronic state and atomic-type

TABLE I. Molecular states of the PH^+ molecule. Note that the excitation energies of P and P^+ are from Ref. [14], and the value of the ionization potential of the P atom is from Ref. [13].

Molecular state no.	Molecular-state designation	Asymptote	Relative asymptotic energy (cm^{-1})
1	$1\ ^2\Sigma^+$	$\text{P}^+(3s^23p^2: ^1D) + \text{H}(1s)$	8 883
2	$2\ ^2\Sigma^+$	$\text{P}^+(3s^23p^2: ^1S) + \text{H}(1s)$	21 576
3	$3\ ^2\Sigma^+$	$\text{P}(3s^23p^3: ^2P^o) + \text{H}^+$	43 821
4	$1\ ^2\Delta$	$\text{P}^+(3s^23p^2: ^1D) + \text{H}(1s)$	8 883
5	$2\ ^2\Delta$	$\text{P}(3s^23p^3: ^2D^o) + \text{H}^+$	36 461
6	$1\ ^2\Pi$	$\text{P}^+(3s^23p^2: ^3P) + \text{H}(1s)$	0
7	$2\ ^2\Pi$	$\text{P}^+(3s^23p^2: ^1D) + \text{H}(1s)$	8 883
8	$3\ ^2\Pi$	$\text{P}(3s^23p^3: ^2D^o) + \text{H}^+$	36 461
9	$4\ ^2\Pi$	$\text{P}(3s^23p^3: ^2P^o) + \text{H}^+$	43 821
10	$1\ ^2\Sigma^-$	$\text{P}^+(3s^23p^2: ^3P) + \text{H}(1s)$	0
11	$2\ ^2\Sigma^-$	$\text{P}(3s^23p^3: ^2D^o) + \text{H}^+$	36 461
12	$1\ ^4\Pi$	$\text{P}^+(3s^23p^2: ^3P) + \text{H}(1s)$	0
13	$1\ ^4\Sigma^-$	$\text{P}^+(3s^23p^2: ^3P) + \text{H}(1s)$	0
14	$2\ ^4\Sigma^-$	$\text{P}(3s^23p^3: ^4S^o) + \text{H}^+$	25 099
15	$3\ ^4\Sigma^-$	$\text{P}^+(3s^13p^3: ^5S^o) + \text{H}(1s)$	45 697
16	$1\ ^6\Sigma^-$	$\text{P}^+(3s^13p^3: ^5S^o) + \text{H}(1s)$	45 697

electron translation factors (ETFs), in which the inclusion of the ETF satisfies the correct scattering boundary condition. The ETF effect at 10 keV/u amounts to about 15% of the total charge transfer cross section. Substituting the total wave function into the time-dependent Schrödinger equation and retaining the ETF correction up to first order in the relative velocity between the collision partners, we obtain a set of first-order coupled equations in time t . Transitions between the molecular states are driven by nonadiabatic couplings. By solving the coupled equations numerically, we obtain the scattering amplitudes for transitions: the square of the amplitude gives the transition probability, and integration of the probability over the impact parameter gives the cross section. The molecular states included in the dynamical calculations are the two sets of states as shown in Fig. 1: (i) quartets; $[\text{H}+\text{P}^+(^3P)]$ ($1\ ^4\Sigma^-, 1\ ^4\Pi$) and $[\text{H}+\text{P}^+(^5S^o)]$ ($3\ ^4\Sigma^-$) states for electron capture from the initial ground $[\text{H}^++\text{P}(^4S^o)]$ ($2\ ^4\Sigma^-$) state, (ii) doublets; $[\text{H}+\text{P}^+(^3P)]$ ($1\ ^2\Sigma^-, 1\ ^2\Pi$), $[\text{H}+\text{P}^+(^1D)]$ ($1\ ^2\Sigma^+, 2\ ^2\Pi$) and $[\text{H}+\text{P}^+(^1S)]$ ($2\ ^2\Sigma^+$) states for electron capture from the initial excited $[\text{H}^++\text{P}(^2D^o)]$ ($2\ ^2\Sigma^-, 3\ ^2\Pi$) states.

RESULTS

Adiabatic potentials and couplings

The molecular states of the PH^+ molecule calculated in the present paper are listed in Table I, together with the atomic designation to which each molecular state separates at infinite internuclear separation and the relative energies above the asymptote of the lowest molecular state. The level of precision of our molecular-state calculations is better than 0.2% for all states in comparison with experimental asymptotic energies [13,14]. The states above the 16th state in Table I are $3\ ^2\Sigma^-, 5\ ^2\Pi, 3\ ^2\Delta, 4\ ^4\Sigma^-, 2\ ^4\Pi$, and $1\ ^4\Delta$, which lie $65\,252\ \text{cm}^{-1}$ above the lowest state in the same table. Figures 1(a) and 1(b) show the adiabatic potentials of the PH^+ molecule listed in Table I for all the related ($^2\Sigma^+$

and $^2\Delta$ states are not shown) states obtained in the present calculation [Fig. 1(a)], and for quartet states [Fig. 1(b)], respectively. As stated, the ground $[\text{H}^++\text{P}(^4S^o)]$ channel is a quartet state, and there are three quartet states energetically nearby, which correspond to $[\text{H}+\text{P}^+(^3P)]$ and $[\text{H}+\text{P}^+(^5S^o)]$ channels. The first metastable excited state is a doublet D state and a few levels nearby belong to this manifold, as seen in the figure. The energy separation between the initial metastable $[\text{H}^++\text{P}(^2D^o)]$ channel and the lowest $[\text{H}+\text{P}^+(^3P)]$ channel coupled is less than 5 eV, and within this energy separation, there are two more doublet channels. Of course, above the initial channel, there are more states packed closely together within a narrow range, which strongly couple with the initial doublet channel. Therefore, it may be rather difficult to obtain a converged result of the cross section for charge transfer from the metastable channel.

Because it is a lowly charged ion-atom system, adiabatic potentials for the quartet manifold show no strong curve crossing, and hence inelastic processes arising from the present collision system are thought to proceed through the Demkov-type mechanism. Representative couplings are illustrated for the quartet manifold in Figs. 2 and 3 for radial and rotational couplings, respectively. As described, the radial couplings shown are relatively weak and have significant values only at small internuclear separations below $\sim 8a_0$. The rotational coupling, which connects to the flux exit for charge-transfer processes, is also weak and of short range. Specific details are discussed separately under each subject below. For the doublet manifold, the initial $3\ ^2\Pi$ state has a strong avoided crossing with the $2\ ^2\Pi$ state at around $3a_0$, and this crossing is expected to result in a large radial coupling between the two states. The $2\ ^2\Delta$ state is seen to possess a real curve crossing with the $3\ ^2\Pi$ state at $2.6a_0$, which may be important for the flux exit. The $3\ ^2\Pi$ state has another avoided crossing with the $4\ ^2\Pi$ state at around $4.8a_0$, which may play a key role for the target excitation process as well as charge transfer processes at higher

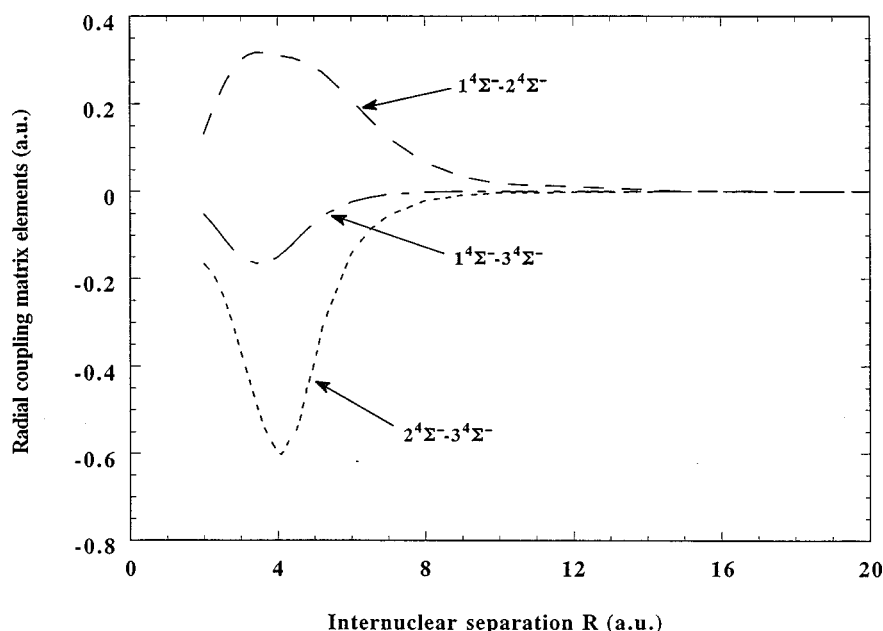


FIG. 2. Representative radial coupling matrix elements for quartet states.

energy. As discussed above, the radial coupling between the $3^2\Pi$ and $2^2\Pi$ has an extremely sharp and large peak at $3.0a_0$ with a peak value of 20.0 a.u. This coupling is expected in principle to play a secondary role in dynamics in the present energy region because of its diabatic nature. That for $3^2\Pi$ and $4^2\Pi$ also exhibits a sharp peak, but to a somewhat lesser extent, at $2.4a_0$ with a value of 1.6 a.u. and it is expected to be more effective for dynamics than the one between the $3^2\Pi$ and $2^2\Pi$. The rotational coupling between the $2^2\Delta$ and $3^2\Pi$ states has a sizable value in the R region where the curve crossing occurs, and hence this coupling is the one that primarily contributes to the dynamics. The initial $2^2\Sigma^-$ has a different symmetry from other Σ states nearby, which have (+) symmetry, and hence the con-

tribution from the $2^2\Sigma^-$ state should be weak except for the lowest $1^2\Sigma^-$ state, which directly couples with $2^2\Sigma^-$.

Charge transfer from the ground $P(^4S^o)$ state

First we consider the collision process (1a) where the target P atom is in its ground state, $P(3s^23p^3: ^4S^o)$. The incoming channel is the $2^4\Sigma^-$ state. As shown in Fig. 1(b), we coupled Nos. 12–15 states in Table I for the calculation of the cross section. Both the radial coupling matrix elements between the incoming channel, $2^4\Sigma^-$, and the outgoing channels, $3^4\Sigma^-$, and $1^4\Sigma^-$, have broad peaks around $R \sim 4.0a_0$ and $3.4a_0$, respectively, and the matrix element between $2^4\Sigma^-$ and $3^4\Sigma^-$ is considerably larger than that be-

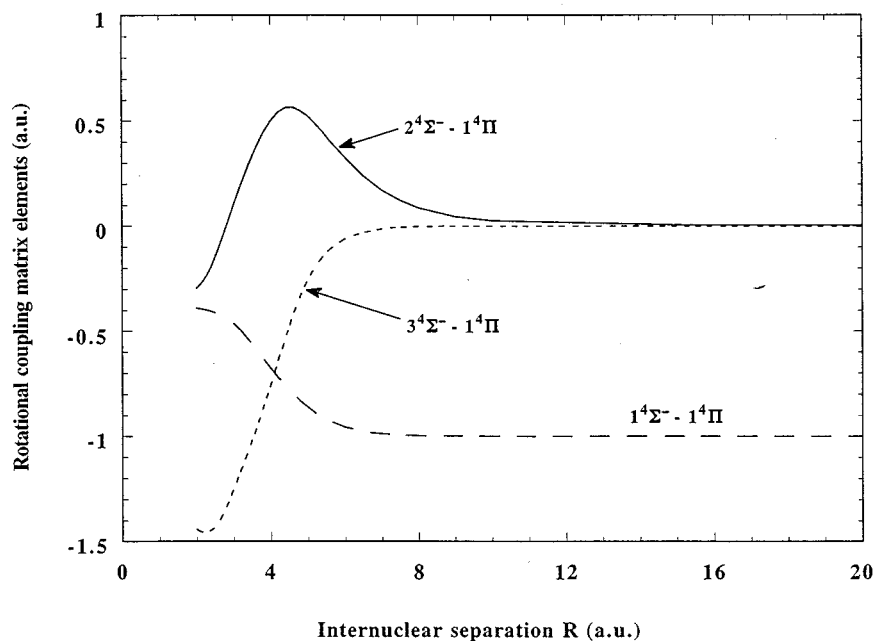
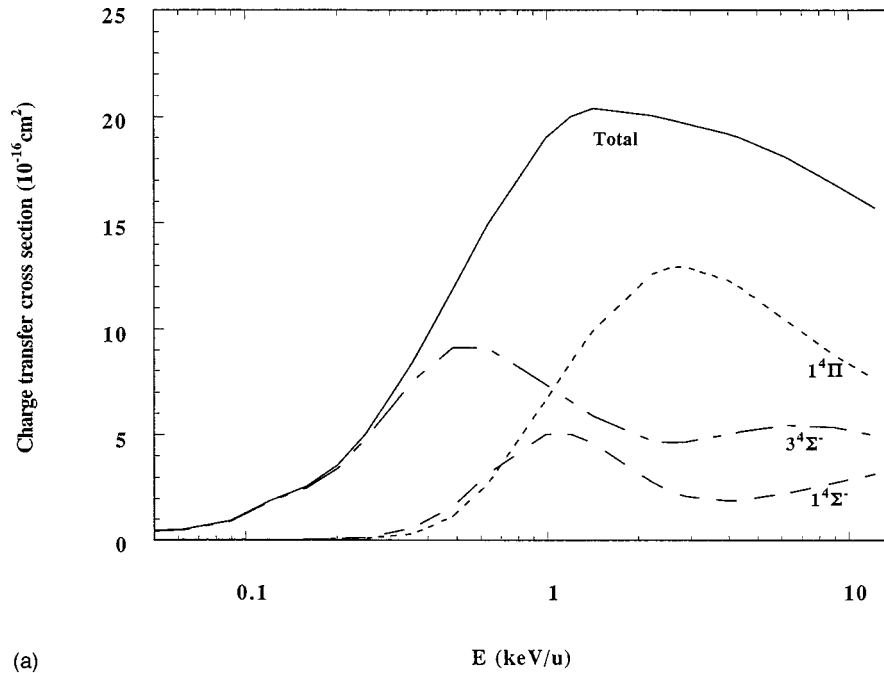
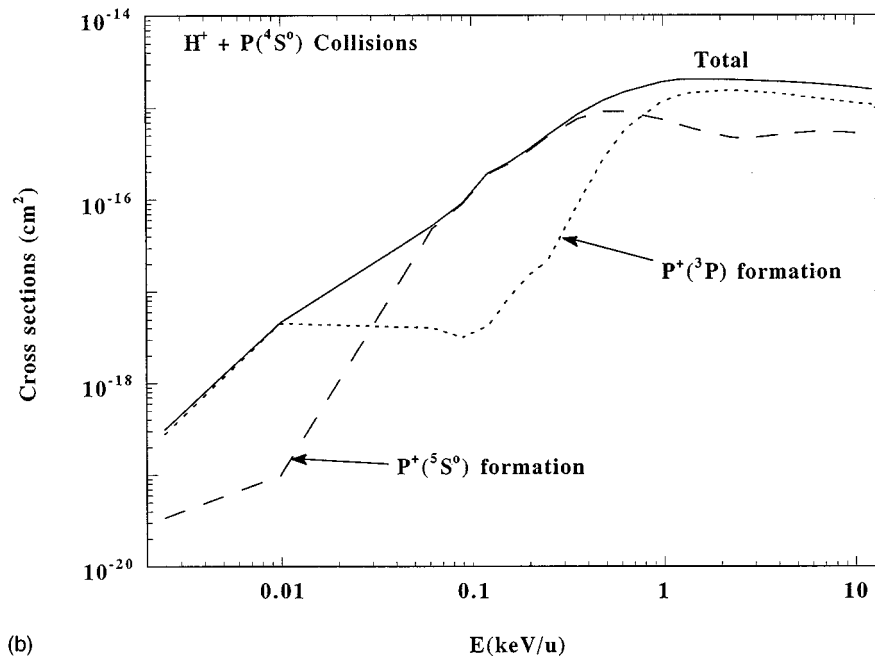


FIG. 3. Representative rotational coupling matrix elements for quartet states.



(a)



(b)

FIG. 4. (a) Contributions from each channel to charge-transfer cross sections from the ground $P(4S^0)$ atom and (b) each ion production cross section and total cross section from the ground state.

tween $2^4\Sigma^-$ and $1^4\Sigma^-$, while the energy gap of the former pair is less than that of the latter. Therefore, at lower energies where the rotational coupling is less effective, we expect the contributions to the charge-transfer cross section from the $3^4\Sigma^-$ channel to dominate. Also, we expect the contribution from the $1^4\Sigma^-$ channel to be the smallest. As the collision energy increases, the rotational coupling becomes more effective, and from Fig. 3 we expect contributions from the $1^4\Pi$ channel to increase. These observations are in accordance with our calculated results shown in Fig. 4(a). In the figure, we include the contribution from each channel. Above 1 keV/u, the Π state is far dominant over other Σ states, but below 1 keV/u, $3^4\Sigma^-$ state, i.e., $P^+(3s^13p^3:5S^0)$ state formation, becomes a strong channel for charge transfer

although below 0.1 keV/u or so, $3^4\Sigma^-$ state takes over. In Fig. 4(b), we show cross sections for ion productions, and see that above ~ 1 keV/u, $P^+(3s^23p^2:3P)$ is produced more efficiently, but as the energy decreases, $P^+(3s^13p^3:5S^0)$ production dominates down to 0.03 keV/u. Below this energy, $P^+(3s^23p^2:3P)$ production takes over again. Around 1 keV/u, both productions are comparable in magnitude. The production of $P^+(3s^23p^2:3P)$ peaks near 1 keV/u, but is small down to 0.02 keV/u.

Charge transfer from the metastable $P(2D^0)$ state

There are three states corresponding to this channel, i.e., (i) $2^2\Sigma^-$, (ii) $3^2\Pi$, and (iii) $2^2\Delta$. For assessing the con-

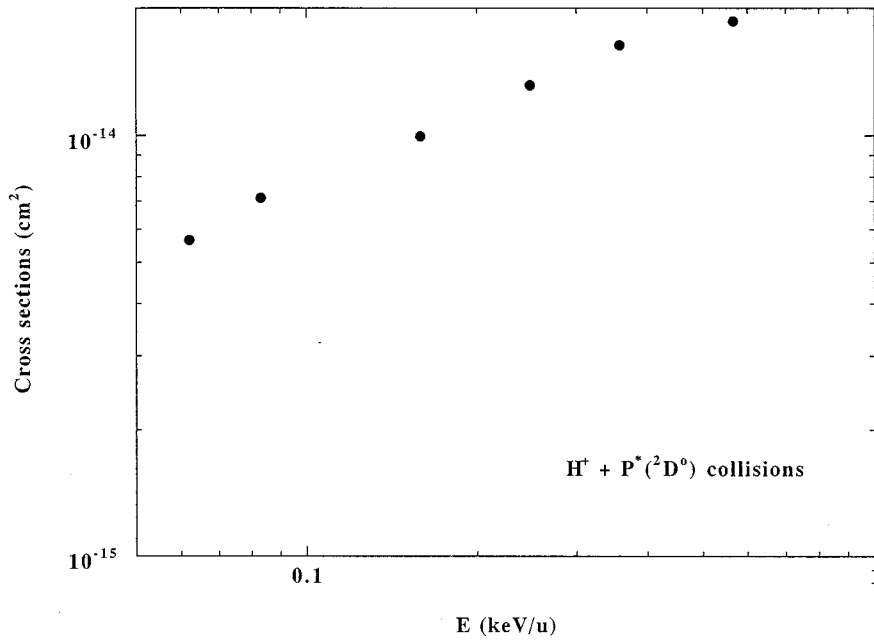


FIG. 5. Charge-transfer cross sections from the metastable $P(^2D^o)$ atoms colliding with H^+ ions.

tribution, we have carried out dynamical calculations for a few energy points from these channels, and discuss the effect briefly below. However, note that the number of channels included is quite limited and no complete convergence of the result was attained. Hence, the results presented are of qualitative significance, rather than quantitative.

Because of the degeneracy among initial $2^2\Sigma^-$, $3^2\Pi$, and $2^2\Delta$ states, most of the flux from each initial channel is mixed before the flux really reaches a strong coupling region for the exit. As seen, there are two strong couplings that connect between the initial $3^2\Pi$ and $2^2\Pi$ states, and between the initial $2^2\Delta$ state and $3^2\Pi$ state at small R , and these couplings indeed play a key role for the transition. As described in the previous section, the radial coupling between the $3^2\Pi$ and $2^2\Pi$ states is not so effective due to the diabatic nature at the collision energy larger than a few 10 eV/u, while the rotational coupling between the $2^2\Delta$ and $3^2\Pi$ states dominates in the entire energy region studied. Hence, the $3^2\Pi$ and $2^2\Sigma^-$ states serve as reservoirs to feed the flux to the $2^2\Delta$ state for the exit, although the $2^2\Sigma^-$ state behaves rather independently because the promotion of the flux to the $2^2\Delta$ state is a two-step mechanism. All radial and rotational couplings from all the initial channels appear to be stronger and more effective to higher levels rather than lower ones, suggesting that we need to include a large number of states from energetically higher levels in order to assure the sufficient convergence of cross sections, as often seen in larger atomic targets. In fact, we have found that this is the case.

The charge-transfer cross section from excited $P(3s^23p^3: ^2D^o)$ atoms is obtained by taking the statistical weight, viz., $\sigma_{\text{ex}} = [\sigma_{\Sigma} + 2\sigma_{\Pi} + 2\sigma_{\Delta}]/5$ (where the subscripts indicate the initial channel above) into account, and the results, along with partial contributions, are illustrated in Fig. 5. As speculated, the higher-lying $4^2\Pi$ state is the dominant contributor that results in target excitation through both the $3^2\Pi$ state and $4^2\Pi$ radial coupling and $2^2\Delta$ state and $4^2\Pi$ rotational coupling at all energies studied. At higher energy, the $3^2\Pi$ state and $4^2\Pi$ radial coupling dominates,

while as the energy decreases, $2^2\Delta$ state and $4^2\Pi$ coupling takes over the dynamics. In addition, $2^2\Sigma^-$ state and $3^2\Sigma^-$ radial coupling is expected to play some part at intermediate energy. Obviously, charge transfer from the metastable atom is much larger than that from the ground state in all energies studied.

CONCLUSIONS

We have investigated charge-transfer processes in the ground [$H^+ + P(^4S^o)$] state and the metastable [$H^+ + P(^2D^o)$] state in the collision energy range from 10 eV/u to 10 keV/u. Total capture cross section from the ground state shows a rather smooth increase with collision energy reaching a maximum at 1–2 keV/u with a magnitude of $2.5 \times 10^{-15} \text{ cm}^2$. The total charge-transfer cross section from the metastable state also appears to slowly increase with the collision energy, with the cross section varying from 5×10^{-15} to $3 \times 10^{-14} \text{ cm}^2$ as the collision energy increases from 50 to 300 eV/u. Although there are three initial channels for the collision from the metastable atom, only the $2^2\Delta$ and $3^2\Pi$ states are found to be main contributors to the dynamics. Millar, Farquhar, and Willacy [15] proposed the rate coefficient for charge transfer for the present process as $1.0 \times 10^{-9} \text{ cm}^3/\text{s}$, which is energy independent. The present value of the rate coefficient is approximately in the order of $10^{-7} \text{ cm}^3/\text{s}$ at 1 keV/u, which is found to be much larger than the value of Millar, Farquhar, and Willacy. The cross-section data provided here will be particularly helpful for further assessing the basic therapeutic potential for heavy-ion treatment for bone tumors.

ACKNOWLEDGMENTS

The work was supported in part by a Grant-in-Aid from the Ministry of Education through Yamaguchi University, by Deutsche Forschungsgemeinschaft in the form of a Forschergruppe and Grant No. Bu450/7-1, and the Robert A. Welch Foundation. The financial support of the Fonds der Chemis-

chen Industrie is also gratefully acknowledged. M.K. acknowledges the support from the Deutscher Akademischer

Austauschdienst (DAAD) through the Universität Wuppertal during the time when much of this paper was written.

-
- [1] *Proceedings of NIRS International Seminar on the Application of Heavy Ion Accelerator to Radiation Therapy of Cancer, Chiba, Japan, 1994*, edited by T. Kanai and E. Takeda (National Institute of Radiological Sciences, Chiba, Japan, 1994).
- [2] J.-P. Gu, G. Hirsch, R. J. Buenker, M. Kimura, C. M. Dutta, and P. Nordlander, *Phys. Rev. A* **57**, 4483 (1998).
- [3] M. Kimura, J.-P. Gu, G. Hirsch, R. J. Buenker, A. Domondon, T. Watanabe, and H. Sato, *Phys. Rev. A* **56**, 1892 (1997).
- [4] M. Kimura, J.-P. Gu, G. Hirsch, and R. J. Buenker, *Phys. Rev. A* **55**, 2778 (1997).
- [5] A. D. McLean and G. S. Chandler, *J. Chem. Phys.* **72**, 5639 (1980).
- [6] T. H. Dunning, Jr. and P. J. Hay, in *Methods of Electronic Structure Theory*, edited by H. F. Schaefer III (Plenum, New York, 1977), p. 1.
- [7] D. E. Woon and T. H. Dunning, Jr., *J. Chem. Phys.* **98**, 1358 (1993).
- [8] J. Römelt, S. Peyerimhoff, and R. J. Buenker, *Chem. Phys.* **34**, 403 (1978).
- [9] R. J. Buenker and S. D. Peyerimhoff, *Theor. Chim. Acta* **35**, 33 (1974); **39**, 217 (1975); R. J. Buenker, *Int. J. Quantum Chem.* **29**, 435 (1986).
- [10] R. J. Buenker, in *Proceedings of the Workshop on Quantum Chemistry and Molecular Physics, Wollongong, Australia*, edited by P. G. Burton (Wollongong University Press, Wollongong, Australia, 1980); in *Studies in Physical and Theoretical Chemistry*, edited by R. Carbo, *Current Aspects of Quantum Chemistry Vol. 21* (Elsevier, Amsterdam, 1981), p. 17; R. J. Buenker and R. A. Phillips, *J. Mol. Struct.: THEOCHEM* **123**, 291 (1985).
- [11] G. Hirsch, P. J. Bruna, R. J. Buenker, and S. D. Peyerimhoff, *Chem. Phys.* **45**, 335 (1980).
- [12] M. Kimura and N. F. Lane, in *Advances in Atomic, Molecular and Optical Physics*, edited by D. Bates and B. Bederson (Academic, New York, 1989), Vol. 26, p. 76.
- [13] S. Baskin and J. D. Stoner, Jr., *Atomic Energy Levels and Gortian Diagram* (North-Holland, Amsterdam, 1975).
- [14] C. E. Moore, *Atomic Energy Levels*, Natl. Bur. Stand. (U.S.) Circ. No. 467 (U.S. GPO, Washington, D.C., 1949), Vol. 1.
- [15] T. J. Millar, P. R. A. Farquhar, and K. Willacy, *Astron. Astrophys., Suppl. Ser.* **121**, 139 (1997).